

## 4. ABSORPTION IN IMPERFECT CRYSTALS

Imperfections in quartz can either modify the intrinsic processes discussed above or create a new absorption of their own.

The reduction of the lifetime  $\theta$  of thermal phonons in imperfect crystals does not influence the synchronous absorption, which is independent of  $\theta$  as long as  $\omega\theta > 1$ . But the nonsynchronous absorption (14) will be enhanced if  $\theta$  is reduced, for example, by impurity scattering. If the scattering rate  $1/\theta$  is now independent of temperature or, as in the case of Rayleigh scattering increasing with temperature, the temperature dependence  $T^4/\theta$  should be at least as steep as  $T^4$ .

The experimental observations on the imperfect and the neutron-irradiated  $X$  cuts of Fig. 4 do not confirm this picture. The extra absorption varies only little with temperature above 10°K, but rapidly disappears below 7°K. A similar step-like behavior of the absorption was

also reported by Jacobsen<sup>10</sup> for an  $AC$  cut. This extra absorption may arise within the imperfect regions of the crystal: Jones<sup>18</sup> *et al.* found recently at 930 Mc/sec in fused quartz an enormous ultrasonic absorption which could only be frozen out at a few degrees Kelvin. This suggests that the imperfections in our  $X$  cut, as well as in the neutron-irradiated sample, are small regions of vitrification with a characteristic high absorption. The size of these imperfect regions has been discussed in Sec. 2.

*Note added in proof.* In a recent experiment on aluminum [Appl. Phys. Letters 3, 195 (1963)], Hikita *et al.* have demonstrated that the anharmonicity of a crystal—as expressed by Grüneisen's constant in our Eqs. (10) and (14)—can be strongly increased by the presence of imperfections as, for example, dislocations.

<sup>18</sup> C. K. Jones, P. G. Klemens, and J. A. Rayne, Phys. Letters 8, 31 (1964).

## Electron-Spin Resonances in Gamma-Ray-Irradiated Aluminum Oxide\*

F. T. GAMBLE,† R. H. BARTRAM, C. G. YOUNG,‡ AND O. R. GILLIAM

*University of Connecticut, Storrs, Connecticut*

AND

P. W. LEVY

*Brookhaven National Laboratory, Upton, New York*

(Received 18 November 1963)

Single crystals of  $\alpha$ -aluminum oxide were subjected to gamma-ray irradiation at 77°K. A single, asymmetric, paramagnetic-resonance absorption was produced with  $g_{\parallel} = 2.012 \pm 0.002$  and  $g_{\perp} = 2.008 \pm 0.002$ , where  $\parallel$  and  $\perp$  are with respect to the  $c$  axis. The line width is about 50 G at 300 and 77°K. The absorption line has been analyzed as a superposition of three Gaussian lines with the isotropic  $g$  values:  $g_1 = 2.020 \pm 0.003$ ,  $g_2 = 2.006 \pm 0.003$ ,  $g_3 = 2.006 \pm 0.003$ . The component lines are tentatively attributed to two types of centers: a trapped hole localized on an anion adjacent to a cation site which is deficient in positive charge, and an electron trapped at an anion vacancy. The cation site may be vacant, or may contain a monovalent or divalent substitutional impurity.

## I. INTRODUCTION

IRRADIATION of single crystals of  $\alpha$ -aluminum oxide by ultraviolet, gamma-ray, reactor and high-energy-electron radiation, or by combinations of these, produces or ionizes lattice defects. These defects are manifested in a variety of ways including electron-spin resonance (ESR). The modified properties of irradiated  $Al_2O_3$  not only are of intrinsic interest, but also provide information about the radiation-damage mechanism; consequently, they have been studied extensively by

measurement of optical absorption spectra,<sup>1-5</sup> long-wavelength neutron scattering cross sections,<sup>6</sup> thermal conductivity,<sup>7</sup> lattice expansion,<sup>8</sup> and thermoluminescence.<sup>9</sup> However, none of these measurements has provided conclusive identification of the underlying cen-

<sup>1</sup> R. A. Hunt and R. H. Schuler, Phys. Rev. 89, 664 (1953).

<sup>2</sup> P. W. Levy and G. J. Dienes, *Report of the Bristol Conference on Defects in Crystalline Solids* (The Physical Society, London, 1955), p. 256.

<sup>3</sup> P. W. Levy, Phys. Rev. 123, 1226 (1961).

<sup>4</sup> E. W. J. Mitchell, J. D. Rigden, and P. W. Townsend, Phil. Mag. 5, 1013 (1960).

<sup>5</sup> G. W. Arnold and W. D. Compton, Phys. Rev. Letters 4, 66 (1960).

<sup>6</sup> J. Antal and A. Goland, Phys. Rev. 112, 103 (1958).

<sup>7</sup> R. Berman, E. L. Foster, B. Schneidmeyer, and S. M. A. Tirmizi, J. Appl. Phys. 31, 2156 (1960).

<sup>8</sup> D. G. Martin, Phys. Chem. Solids 10, 64 (1955).

<sup>9</sup> A. F. Gabrysh, H. Eyring, V. LeFebvre, and M. D. Evans, J. Appl. Phys. 33, 3389 (1962).

\* This research was supported by the U. S. Atomic Energy Commission.

† Present address: Department of Physics and Astronomy, Denison University, Granville, Ohio.

‡ Present address: American Optical Company, Southbridge, Massachusetts.

ters, which is fundamental to an understanding both of the properties of irradiated  $\text{Al}_2\text{O}_3$  and of the damage mechanism. This paper describes ESR measurements on gamma-ray-irradiated  $\text{Al}_2\text{O}_3$  and includes tentative identification of several centers. Preliminary results of this study have been reported previously.<sup>10,11</sup> ESR measurements on reactor- and electron-irradiated  $\text{Al}_2\text{O}_3$  have also been made and will be reported separately.

After a single crystal of  $\text{Al}_2\text{O}_3$  has been exposed to gamma-ray irradiation, a single, asymmetric, paramagnetic-resonance line is observed with an anisotropic  $g$  value slightly greater than the free-electron value. The asymmetry becomes more pronounced when the microwave power is reduced and also when the absorption line is partially annealed. The resonance line has been analyzed into three Gaussian components which are believed to be caused by the ionization of existing defects in the crystal.

## II. CRYSTAL STRUCTURE

The basic crystal structure of  $\alpha\text{-Al}_2\text{O}_3$ , or corundum, is rhombohedral. The space group assigned is  $D_{3d}^6$  ( $R\bar{3}c$ ).<sup>12</sup> Bersohn<sup>13</sup> has concluded that the bonding is predominantly ionic on the basis of field gradient calculations. Laurance<sup>14</sup> *et al.* have postulated a 20% covalent character to the bonds, based on calculations using Pauling's<sup>15</sup> formula relating the electronegativity difference to the degree of covalency. Their interpretation of ENDOR measurements on  $\text{Al}_2\text{O}_3$  appears to confirm this assumed bond character.

The crystal may be viewed as a hexagonal close packing of oxygen ions ( $\text{O}^{2-}$ ) with pairs of aluminum ions ( $\text{Al}^{3+}$ ) at interstitial sites along the crystalline  $c$  axis sharing equilateral triangles of oxygen ions between them. Electrostatic forces between the  $\text{Al}^{3+}$  and  $\text{O}^{2-}$  ions reduce the size of the shared triangles and produce a slight distortion in the hexagonal close packing. This contraction results in a slight enlargement and rotation about the  $c$  axis of the adjoining triangles which consist of oxygen ions from three adjacent coplanar molecules. Rotation in both senses occur in equal numbers throughout the lattice. Recent measurements of the  $\alpha\text{-Al}_2\text{O}_3$  structure by Newnham and deHaan yield a value of  $3.9^\circ$  for this angle of rotation.<sup>16</sup> Figure 1 is a perspective view of three coplanar  $\text{Al}_2\text{O}_3$  molecules and indicates this rotation and enlargement. Above and below the center of the rotated triangle are interstices of the hexa-

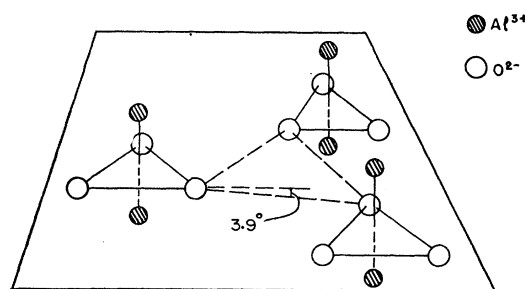


FIG. 1. Perspective view of three adjacent, coplanar,  $\text{Al}_2\text{O}_3$  molecules.

gonal close packing of oxygens. Either the interstice above or the one below is occupied by an aluminum ion. Such an ion is not shown in Fig. 1, since it is associated with a molecule whose plane of oxygen ions lies above or below the plane of the triangle.

An alternative approach, which more clearly indicates certain local symmetries along the  $c$  axis, is to view each aluminum ion as residing in a slightly distorted octahedron of 6 oxygen ions. Three of the oxygen ions are those of a molecule while the remaining three are those of a "rotated" triangle. Every third octahedral interstice along the  $c$  axis is a natural void with both triangles rotated in the same sense. The point symmetry is  $C_3$  at the aluminum site,  $C_{3i}$  at the void,  $D_3$  at the center of an  $\text{Al}_2\text{O}_3$  molecule, and  $C_2$  at an oxygen site.

## III. EXPERIMENTAL DETAILS

The aluminum-oxide single crystals, which were obtained from the Linde Company, were grown by the Verneuil process. They were cut and polished to optical flats, approximately 20 mm by 10 mm by 1 mm, with the crystalline  $c$  axis normal to the flat. All of the unirradiated crystals showed prominent background spectra of  $\text{Fe}^{3+}$  and  $\text{Cr}^{3+}$  resonances; however, the impurity content of different crystals differed by an order of magnitude. Since impurity analyses on the crystals have not been performed, the presence of other impurities is not known. Estimates by the Linde Company of the impurity concentrations in the starting oxide powders have been published by Gibbs.<sup>17</sup>

Gamma-ray irradiations were made at 77°K in calibrated tubular  $\text{Co}^{60}$  sources at the University of Connecticut and at the Brookhaven National Laboratory (BNL). The observations were made with an X-band superheterodyne paramagnetic resonance spectrometer with 100-cps magnetic field modulation. Rectangular  $TE_{102}$  cavities were employed for all measurements. Cavity design permitted sample loading and unloading at 77°K and incorporated 0.025-in.-diam lead wire "O" ring seals to permit removal of liquid nitrogen and evacuation of the cavity following assembly.

<sup>17</sup> P. Gibbs, in *Kinetics of High Temperature Processes*, edited by W. D. Kingery (John Wiley & Sons, Inc., New York, 1959), p. 26.

<sup>10</sup> O. R. Gilliam, C. G. Young, and P. W. Levy, *Bull. Am. Phys. Soc.* **6**, 117 (1961).

<sup>11</sup> O. R. Gilliam and C. G. Young, 1962 Conference Radiation Effects on Glass, Rochester, New York (unpublished).

<sup>12</sup> R. W. G. Wyckoff, *Crystal Structures* (Interscience Publishers, Inc., New York, 1948), Vol. II.

<sup>13</sup> R. Bersohn, *J. Chem. Phys.* **29**, 326 (1958).

<sup>14</sup> N. Laurance, E. C. McIrvine, and J. Lambe, *Phys. Chem. Solids* **23**, 515 (1962).

<sup>15</sup> L. Pauling, *The Nature of the Chemical Bond* (Cornell University Press, Ithaca, 1960).

<sup>16</sup> R. E. Newnham and Y. M. de Haan, *Z. Krist.* **117**, 235 (1962).

Relative intensity measurements were made using an iron impurity line in an unirradiated aluminum oxide crystal. This calibration sample was cut such that the resonance line used was well separated from the radiation-induced lines. For a determination of the number of spins associated with a center, the sapphire calibration sample was calibrated against DPPH and charred dextrose calibration standards.<sup>18</sup> A microwave frequency standard and a nuclear resonance probe were employed to make precision measurements of frequency and magnetic field, respectively.

#### IV. EXPERIMENTAL RESULTS

Gamma-ray irradiation of  $\text{Al}_2\text{O}_3$  at 77°K produces a single, asymmetric, anisotropic resonance line about 50 G wide with  $g_{\parallel} = 2.012 \pm 0.002$  and  $g_{\perp} = 2.008 \pm 0.002$ , where  $\parallel$  and  $\perp$  refer to the orientation of the magnetic field with respect to the crystal  $c$  axis. These values were obtained prior to annealing on a crystal which had received a gamma-ray dose of  $1.4 \times 10^6 \text{R}$  at 77°K. For these measurements the microwave frequency was 8.9 kMc/sec and the microwave power was about 12 mW. A resonance line was observed with the same width and  $g$  values, but with lower intensity, at room temperature following a room-temperature gamma-ray irradiation. During the observations the spectrometer was operated at power levels as low as  $3 \mu\text{W}$  to preclude the oversight of a power-saturated absorption spectrum.

For irradiations at 77°K, a dose of about  $3 \times 10^4 \text{R}$  of  $\text{Co}^{60}$  gamma rays saturates the growth of the resonance at about  $4 \times 10^{15}$  spins per cubic centimeter, as shown in Fig. 2. Irradiation doses up to  $10^7 \text{R}$  produce no appreciable further increase in intensity. The saturation dose of gamma rays is the same as that reported by Levy for growth saturation of the optical-absorption spectrum<sup>3</sup> and that reported by Berman *et al.* for the change in thermal conductivity in synthetic sapphire.<sup>7</sup> Also, the number of centers is in order-of-magnitude agreement with that reported by Hunt and Schuler

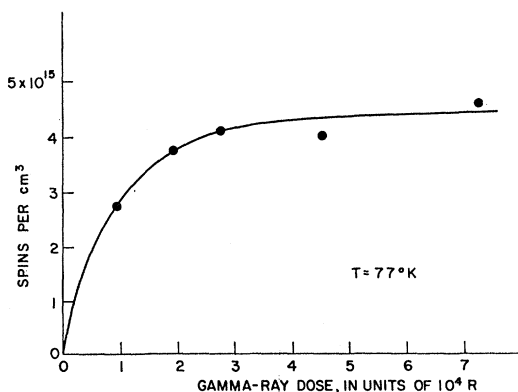


FIG. 2. Growth behavior of gamma-induced ESR line in  $\text{Al}_2\text{O}_3$ .

<sup>18</sup> R. C. Pastor and R. H. Hoskins, *J. Chem. Phys.* **32**, 264 (1960).

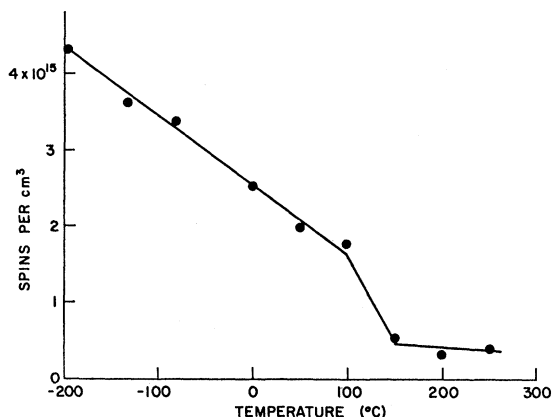


FIG. 3. Stepwise annealing curve of gamma-ray-induced ESR absorption in  $\text{Al}_2\text{O}_3$  for a 30-min anneal at each temperature indicated. This curve represents the annealing of the total number of observed spins without regard to the type of center. Measurements were made at a microwave power of 6 mW.

from optical measurements.<sup>1</sup> A similar absorption line was observed after ultraviolet irradiation with an unfiltered high-pressure mercury vapor lamp, but it has not been studied in detail. The growth saturation behavior, as well as the low-photon energy required to cause the ESR absorption, suggests either that the resonance is due to ionization which takes place at the site of a structural defect, or that it is associated with impurities in the crystal. The intensity of resonance absorption appears approximately the same for crystals with different known-impurity content ( $\text{Fe}^{3+}$  and  $\text{Cr}^{3+}$ ). On the other hand, straining an aluminum-oxide rod by stretching it several percent caused no spin-resonance signal prior to irradiation or any enhancement of the resonance produced by the irradiation, although this procedure might be expected to increase the number of structural defects.

A simple annealing study was conducted on a gamma-ray-irradiated  $\text{Al}_2\text{O}_3$  sample by stepwise 30-min anneals at temperatures up to 250°C. The crystal had received a dose of  $10^6 \text{R}$  of  $\text{Co}^{60}$  gamma rays at liquid-nitrogen temperature. The relative intensity of the absorption after each anneal was determined by several ESR recordings at 77°K, with the irradiated sample and the unirradiated  $\text{Al}_2\text{O}_3$  calibration sample in the same cavity. A double integration of the derivative curves yielded the relative intensities indicated, which were then plotted as a stepwise annealing curve in Fig. 3. Three annealing stages are apparent. First, there is an approximately linear decay to about 100°C, where a more rapid annealing stage commences. During this latter stage the width of the absorption decreases, contributing to the change in line shape which is described in the next section. Following the 150°C anneal, a hard component or residue appears to remain. After annealing to 250°C, the original line can be restored by gamma-ray irradiation. No bleaching by roomlight was observed during these annealing operations.

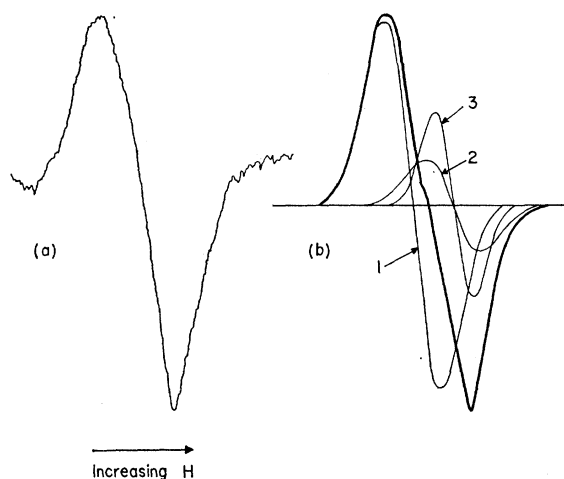


FIG. 4. (a) Gamma-ray-induced resonance line in  $\text{Al}_2\text{O}_3$  at  $\theta=170^\circ$ ,  $\phi=90^\circ$ . In Figs. 4-7, the magnetic-field orientation is specified with respect to the  $c$  axis as polar axis. (b) Resolution into component Gaussian derivatives.

The shape of the gamma-ray-induced resonance line varies appreciably with orientation of the magnetic field and with microwave power level. It was found that the shape could be represented moderately well by a superposition of three Gaussian derivatives. This decomposition is illustrated in Figs. 4, 5, and 6 for three different orientations of the magnetic field. In addition, line shape was seen to change significantly after partial annealing; the decomposition of such a line is shown in Fig. 7. Each component line can be characterized by its  $g$  value, width, and relative amplitude. The parameters of the components of the lines shown in Figs. 4-7 are tabulated in Table I. The line shape was also recorded at a large number of intermediate angles and was found to change continuously and in a manner consistent with the interpretation presented in Sec. V. In addition, a number of lines were repeated several times at a fixed orientation to establish the reproducibility of the line

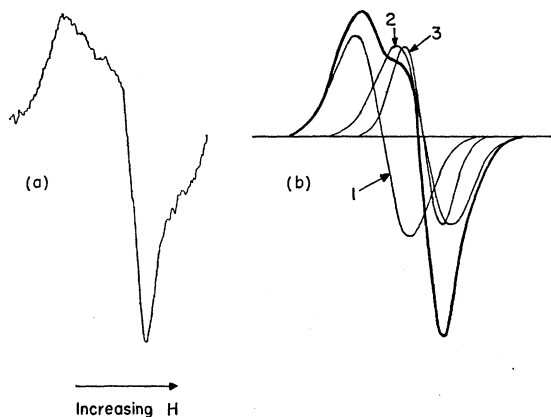


FIG. 5. (a) Gamma-ray-induced resonance line in  $\text{Al}_2\text{O}_3$  at  $\theta=90^\circ$ ,  $\phi=90^\circ$ . (b) Resolution into component Gaussian derivatives.

shape. The lines shown in Figs. 4-7 were selected for good signal-to-noise ratio and minimum interference from impurity spectra. The best signal-to-noise ratio was about 20, a consequence of the very small number of centers and the large line breadth. Line shapes identical to those analyzed were obtained on several samples; however, other samples showed somewhat different line shapes, the difference apparently corresponding to a change in the relative amplitude of component 3.

It can be seen from Table I that in every case it was possible to impose the following constraints on the components: (1) Components 1 and 2 have the same width. (2) Components 2 and 3 have the same  $g$  values. (3) The difference in the  $g$  values of components 1 and 2 is 0.0147. (It should be noted that this resolution is not necessarily unique; it may be possible to find components which do not satisfy the constraints.)

Within experimental error, the  $g$  values of the components are independent of magnetic-field orientation, microwave power level, and annealing. The anisotropy of

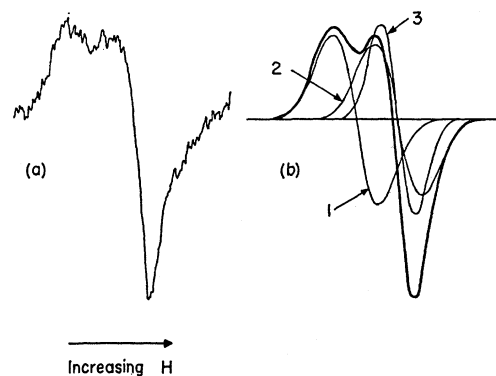


FIG. 6. (a) Gamma-ray-induced resonance line in  $\text{Al}_2\text{O}_3$  at  $\theta=90^\circ$ ,  $\phi=145^\circ$ . (b) Resolution into component Gaussian derivatives.

the  $g$  value of the composite line appears to be due entirely to the changes in relative amplitudes of the three components; thus, the ratio of amplitudes of components 1 and 2 is 4.00 when the magnetic field is  $10^\circ$  from the  $c$  axis as in Fig. 4, but only 1.12 when the field is perpendicular to the  $c$  axis as in Figs. 5 and 6. The difference in shape between Figs. 5 and 6 is attributed to microwave power saturation effects. At  $\phi=90^\circ$ , corresponding to Fig. 5, the rf and dc magnetic fields are perpendicular. At  $\phi=145^\circ$ , corresponding to Fig. 6, the rf and dc magnetic-field directions differ by  $35^\circ$  and there is a reduction in transition probability equivalent to a power reduction of 6 dB at a fixed angle. This causes a change in line shape which is qualitatively the same as that observed when the power is reduced at a fixed angle. Note that apart from this effect, the line shape should repeat every  $60^\circ$  in azimuth in a plane perpendicular to the  $c$  axis by virtue of the trigonal symmetry and inversion symmetry of the crystal and should therefore look nearly the same at  $\phi=90^\circ$  and  $\phi=145^\circ$ .

In fact, the entire azimuthal variation of the composite line can be accounted for by power saturation. It can be seen from Table I and from the figures that the widths of all three components in Fig. 6 are reduced from their values in Figs. 4 and 5; further, the relative amplitude of component 3 in Fig. 6 is enhanced when compared with Fig. 5, while components 1 and 2 have the same relative amplitudes as in Fig. 5.

The resonance line shown in Fig. 7 was obtained by gamma-ray irradiating a sample at 77°K and then subjecting it to a series of stepwise anneals of 30-min duration at temperature intervals of approximately 50°C terminated at 150°C. The sample was returned to 77°K for measurement. Although for Fig. 7 the line was measured at full power, the widths of the components are reduced. The amplitude ratio of components 1 and 2 is 1.33 at  $\theta=110^\circ$ , which is close to the value 1.12 ob-

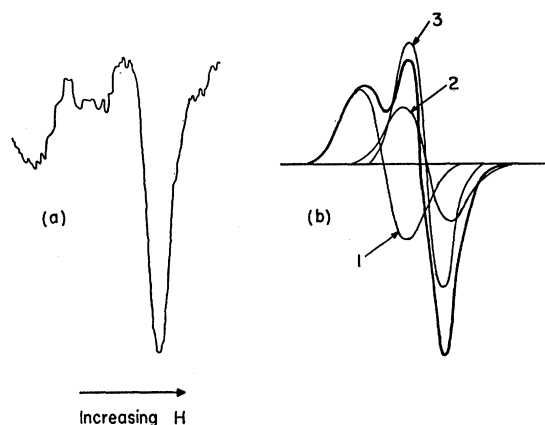


FIG. 7. (a) Gamma-ray-induced resonance line in  $\text{Al}_2\text{O}_3$  at  $\theta=110^\circ$ ,  $\phi=90^\circ$ , following a series of 30-min-stepwise anneals at approximately 50°C intervals terminating at 150°C. (b) Resolution into component Gaussian derivatives.

TABLE I. A choice of  $g$  values, widths, and relative amplitudes of Gaussian components which fit the spin-resonance spectra shown in Figs. 4-7. The  $g$  value of each component is independent of the orientation of the magnetic field within experimental error.

Figure	$\theta$	$\phi$	Component	$g$	Width in gauss	Relative amplitude
4	170°	90°	1	2.0187	30	4.00
			2	2.0040	30	1.00
			3	2.0040	20	2.00
5	90°	90°	1	2.0209	30	1.12
			2	2.0062	30	1.00
			3	2.0062	30	1.00
6	90°	145°	1	2.0203	25	1.12
			2	2.0056	25	1.00
			3	2.0056	17.5	1.25
7	110°	90°	1	2.0213	25	1.33
			2	2.0066	25	1.00
			3	2.0066	17.5	2.16
Average $g$ values			1	2.020		
			2	2.006		
			3	2.006		

tained at  $\theta=90^\circ$  from Fig. 5, but the relative amplitude of component 3 is greatly enhanced by comparison with the unannealed spectrum of Fig. 5. It can be seen from Fig. 3 that the total number of spins was sharply reduced by the anneal at 150°C. The change in line shape also occurred abruptly at this temperature, and no further change in shape was noted after annealing at higher temperatures.

The resonance line was also observed with less than the saturation dose of gamma rays, but there was no apparent change of shape from the resonance line obtained with a saturation dose. Measurements at 4.2°K reveal a single, slightly asymmetric line with  $g=2.008\pm 0.002$  and with a width of 22 G which does not appear to coincide with any of the three components observed at 77°K. These three components are believed to be power saturated at 4.2°K, while the single line observed at 4.2°K is probably obscured at 77°K.

Although the decomposition of the gamma-induced resonance line into three Gaussian derivatives is reasonably convincing, the fit is far from perfect. This is attributable in part to the poor signal-to-noise ratio resulting from the relatively small number of centers and large linewidth, and to instrumental distortion.

## V. DISCUSSION

Prior to irradiation, no paramagnetic resonance centers were observed in the  $\text{Al}_2\text{O}_3$  samples other than those associated with the impurities  $\text{Fe}^{3+}$  with  $S=\frac{5}{2}$  and  $\text{Cr}^{3+}$  with  $S=\frac{3}{2}$ . In the lattice host ions, namely,  $\text{Al}^{3+}$  and  $\text{O}^{2-}$ , all electronic spins are paired. On the other hand, the saturation with dose of the single, asymmetric line induced by gamma irradiation indicates that it arises from the ionization of initially-present defects in the crystal. Thus there is indirect evidence for the presence of defects in the form of diamagnetic centers in unirradiated crystals. In this section we will propose a model for the defects, and the centers formed by gamma-ray irradiation, which accounts fairly well for the ESR data.

It is proposed that the initially present defects include cation sites which are deficient in positive charge, by virtue either of being vacant or of containing monovalent or divalent substitutional impurities in their highest oxidation states. In addition, it is proposed that at least some of these defects are compensated by anion vacancies. Such defects would not exhibit spin resonance in the absence of trapped charges. Gamma-ray irradiation then creates electron-hole pairs, and some of the electrons are trapped at anion vacancies while the corresponding holes are trapped at the charge-deficient cation sites. This process is equivalent to the transfer of electrons from charge-deficient cation sites to remote anion vacancies, as shown in Fig. 8. For the sake of clarity, in the following discussion the charge-deficient cation sites will be referred to as cation vacancies, al-

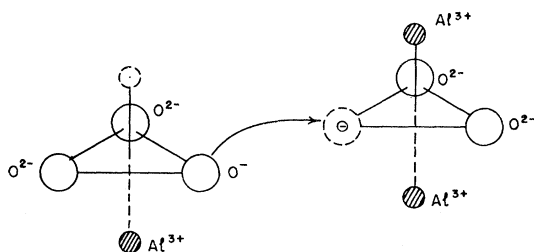


Fig. 8. Proposed mechanism for the effect of gamma-ray irradiation on  $\text{Al}_2\text{O}_3$ . An electron is removed from an anion adjacent to a charge-deficient cation site and transferred to a remote anion vacancy. The charge-deficient cation site may be vacant, or may contain a monovalent or divalent substitutional impurity.

though it should be apparent that the explanation will work just as well if the sites contain monovalent or divalent substitutional impurities.

In order to account for part of the asymmetry of the observed ESR spectrum, it is assumed that a hole trapped at a cation vacancy is localized on a neighboring anion for at least  $10^{-9}$  sec. Similar hole localization was required by Wertz *et al.*<sup>19,20</sup> in analyzing the spectrum of irradiated MgO. The resulting center can then be described as an  $\text{O}^-$  ion, which has spin  $\frac{1}{2}$ , in a strong axial field due to the neighboring cation vacancy. The hole occupies a  $2p$  orbital, and the threefold orbital degeneracy is removed by the axial field, leaving an orbital singlet and an orbital doublet. Since the cation vacancy appears as a negative charge, the hole has a lower energy when it occupies the  $2p$  orbital which is directed toward the vacancy than when it occupies the two perpendicular orbitals; consequently, the orbital singlet lies lowest. In this circumstance, the components of the  $g$  tensor are given by

$$\mathbf{g}_{\parallel} = g_e, \quad (1a)$$

$$\mathbf{g}_{\perp} = g_e(1 - \lambda/\Delta), \quad (1b)$$

where  $g_e$  is the free-electron  $g$  value,  $\lambda$  is the spin-orbit coupling constant for  $\text{O}^-$  ( $\lambda < 0$ ),  $\Delta$  is the energy separation of the orbital singlet and doublet, and  $\parallel$  and  $\perp$  are with respect to the line joining the  $\text{O}^-$  ion and the cation vacancy. The symbol  $\mathbf{g}_{\parallel}$  and  $\mathbf{g}_{\perp}$  in Eqs. (1) are given in boldface to avoid confusion with the  $g$  values of the composite line, referred to previously, which are specified with respect to the direction of the crystal  $c$  axis.

Since each cation has six neighboring anions, there are six inequivalent sites for a single hole trapped at a cation vacancy, or a total of twenty-four since there are four inequivalent cation sites. However, only twelve of these sites are distinguishable since the crystal has a center of inversion at a natural void and the spin Hamiltonian is invariant under inversion. Analysis of the data is complicated not only by the multiplicity of

inequivalent sites, but also by the linewidth of the observed spectrum; the widths of the components of the gamma-induced line in  $\text{Al}_2\text{O}_3$  are about 30 G. In  $\text{Al}_2\text{O}_3$  it is believed that  $\mathbf{g}_{\perp} - \mathbf{g}_{\parallel}$  is comparable to the linewidth; accordingly, the observed spectrum consists of a single, asymmetric line composed of twelve components corresponding to different inequivalent sites and with  $\mathbf{g}$  values lying between  $\mathbf{g}_{\parallel}$  and  $\mathbf{g}_{\perp}$ . In order to facilitate analysis of the spectrum, we assume that this composite line can be approximated by a sum of just two components of the same width, one near  $\mathbf{g}_{\parallel}$  and one near  $\mathbf{g}_{\perp}$ . If the magnetic  $z$  axes were distributed isotropically, the amplitude of the component near  $\mathbf{g}_{\perp}$  would be just twice that near  $\mathbf{g}_{\parallel}$ ; if these axes were confined to a plane perpendicular to the crystal  $c$  axis, but isotropically distributed within this plane, then when the magnetic field is perpendicular to the  $c$  axis the two components would have equal amplitude and when the magnetic field is parallel to the  $c$  axis, the component near  $\mathbf{g}_{\parallel}$  would vanish.

Components 1 and 2 of the observed spectrum are identified with single holes trapped at cation vacancies, since they have the same width and their  $g$  values are constant. A comparison of the relative amplitudes at  $\theta = 170^\circ$ , Fig. 4, and  $\theta = 90^\circ$ , Figs. 5 and 6, shows that the distribution of axes lies somewhere between the two hypothetical cases considered above, with the axes favoring an orientation perpendicular to the  $c$  axis. With reference to the discussion of crystal structure above, each aluminum ion lies between two triangles of oxygen ions, one of the compact variety associated with a molecule and the other enlarged and rotated. The compactness of the former triangle is presumably due in part to the attraction of the aluminum ion in question; in its absence, the triangle would enlarge. The resulting distorted octahedron of oxygen ions surrounding the cation vacancy is substantially compressed along the  $c$  axis in agreement with the observed distribution of axes. It follows that  $g_1$  and  $g_2$  are approximately equal to  $\mathbf{g}_{\perp}$  and  $\mathbf{g}_{\parallel}$ , respectively, and therefore from Eqs. (1) and the measured  $g$  values of components 1 and 2 we can infer a value for  $\lambda/\Delta$ :

$$\lambda/\Delta = (\mathbf{g}_{\parallel} - \mathbf{g}_{\perp})/g_e \approx 0.0073. \quad (2)$$

The possibility of two holes being trapped at a single cation vacancy was also considered. If two holes were trapped, presumably they would adopt antipodal positions with respect to the vacancy by virtue of their electrostatic repulsion; the separation of two such oxygen sites is 4.19 Å. If the spins were assumed to act independently, the magnitude of their magnetic-dipole interaction would be of the order of  $\beta/r^3$ , where  $\beta$  is the Bohr magneton and  $r$  is the separation of the spins. This quantity is 125 G, considerably greater than the observed linewidth. Another possibility is that the  $\text{O}^-$  wave functions overlap to the extent that the spins are coupled. In this case, the resultant spin would be zero

<sup>19</sup> J. E. Wertz, P. Auzins, J. H. E. Griffiths, and J. W. Orton, *Discussions Faraday Soc.* **28**, 136 (1959).

<sup>20</sup> J. E. Wertz, J. W. Orton, and P. Auzins, *Discussions Faraday Soc.* **30**, 140 (1961).

or one. It is clear that neither of these possibilities could account for any part of the observed spectrum.

Since component 3 has an isotropic  $g$  value close to the free-electron value and is more readily power saturated, it is tentatively attributed to an electron which is trapped at an anion vacancy and whose spectrum is broadened by unresolved hyperfine interaction with the four neighboring aluminum nuclei. This assignment is not ruled out by the positive value of  $\Delta g$ , viz.,  $+0.004$ , since Wertz *et al.* have observed spectra with positive  $\Delta g$  in MgS, CaS, SrS, MgSe, CaSe, and SrSe which they also ascribe to single electrons trapped at anion vacancies, or "*F* centers" in their nomenclature.<sup>20</sup> These anomalous  $g$  shifts are so far unexplained.

It is interesting to speculate about the changes in line shape that occur when the sample is partially annealed. The fact that the spectrum can be restored by gamma-ray irradiation after annealing to 250°C indicates that annealing at this temperature involves only the transfer of charges rather than the elimination of defects. This is in accord with the annealing behavior of the optical absorption spectra reported by Levy.<sup>21</sup> The amplitude ratio of components 1 and 2, 1.33, seems appropriate for  $\theta=110^\circ$ . The relative amplitude of component 3, however, is greatly enhanced, indicating that the number of holes is reduced faster than the number of electrons. In all of the spectra which were analyzed, the number of holes exceeds the number of electrons; a possible explanation for the discrepancy is that some anion vacancies trap two electrons forming a center with spin zero. Theoretical work in progress indicates that an anion vacancy in  $\text{Al}_2\text{O}_3$  constitutes a deep trap for one or two

electrons. If annealing is accomplished by liberation of holes trapped at cation vacancies, the holes would tend to be repelled by anion vacancies with one trapped electron, which are positive centers, and consequently would preferentially anneal two-electron centers. Consequently the numbers of trapped holes and single trapped electrons would tend to equalize as annealing progressed. The trapped holes may also be tightly bound, leading to the alternative possibility that annealing is accomplished by the liberation of electrons and holes on shallow traps associated with impurities; however, no new impurity ESR spectra or changes in existing impurity spectra have been observed during annealing of the gamma-ray induced absorption. The apparent absence of new spectra may be due to excessive linewidth.

Although it was assumed for the sake of clarity in the previous discussion that the initially-present defects were cation and anion vacancies, an equally plausible alternative is that they consist of monovalent or divalent substitutional impurities which occupy aluminum sites, and at least some of which are stabilized by anion vacancies. Components 1 and 2 could then be attributed to a hole trapped at such an impurity and localized on a neighboring anion. As before, component 3 could be attributed to a single electron trapped at an anion vacancy. The fact that samples containing widely different quantities of known impurities,  $\text{Fe}^{3+}$  and  $\text{Cr}^{3+}$ , showed gamma-ray-induced absorptions of the same intensity casts doubt on this alternative assignment. On the other hand, as noted previously, it was not possible to increase the intensity of the absorption by straining the crystal, although this procedure might be expected to increase the number of vacancies.

<sup>21</sup> P. W. Levy, Discussions Faraday Soc. **31**, 118 (1961).